

Optical phonons in $\text{Al}_x\text{Ga}_{1-x}\text{As}$: Raman spectroscopy

D. J. Lockwood* and Z. R. Wasilewski

Institute for Microstructural Sciences, National Research Council, Ottawa, ON, Canada K1A 0R6

(Received 22 June 2004; published 5 October 2004)

A detailed investigation was made using Raman spectroscopy of the longitudinal and transverse optical phonons in the disordered alloy $\text{Al}_x\text{Ga}_{1-x}\text{As}$ at room temperature. Spectra obtained for a large number of x values were peak fitted to yield the optical phonon band parameters as a function of x . New expressions are obtained for the frequency variation with Al composition for the GaAs-like and AlAs-like modes, as well as the variations in linewidth, line asymmetry, and intensity for the two longitudinal modes. The results when compared with theoretical predictions indicate a need for further theoretical study.

DOI: 10.1103/PhysRevB.70.155202

PACS number(s): 78.30.Fs, 63.50.+x

I. INTRODUCTION

Next to $\text{Si}_{1-x}\text{Ge}_x$, $\text{Al}_x\text{Ga}_{1-x}\text{As}$ is probably the most widely studied semiconductor alloy system. This is primarily because of its scientific and technological importance but also because it is easy to prepare thick layers of $\text{Al}_x\text{Ga}_{1-x}\text{As}$ of any composition on GaAs.^{1,2} The lattice constants of GaAs and AlAs are very similar and thus epilayer growth of their alloy on themselves can proceed with little regard for strain effects.^{1,2}

The Raman and infrared spectra of $\text{Al}_x\text{Ga}_{1-x}\text{As}$ have been studied often in the past, beginning with the infrared work of Illegems and Pearson in 1970.³ A summary of all results obtained up to 1992 from bulk crystals, thick epilayers, and thin epilayers has been given by Jusserand.⁴ The most recent studies since then were by Feng *et al.*⁵ in 1993 and Solomon *et al.*⁶ in 1994, who both used Raman spectroscopy.

It is known from earlier experimental and theoretical studies of III-V mixed compounds of the type $\text{B}_x\text{A}_{1-x}\text{C}$ that the small wave vector optical phonons may exhibit either one- or two-mode behavior.⁷ In one-mode behavior, the phonons of compound AC evolve continually in approximately linear fashion to those of compound BC with increasing concentration x . In two-mode behavior, the vibrational modes of compound AC merge closer with increasing x eventually forming the localized vibrational mode of atom A in compound BC at the limit $x=1$. The obverse is true for the modes of compound BC, which reach the localized mode of atom B in compound AC in the limit $x=0$. A prediction as to which behavior is observed in a given III-V alloy system is not easily obtained, because of the complexity of the phonons in such systems. Indeed, some mixed crystals can exhibit both kinds of behavior at different concentrations.⁷ The infrared and Raman spectral study of $\text{Al}_x\text{Ga}_{1-x}\text{As}$ by Kim and Spitzer⁸ showed very clearly that this III-V disordered system exhibits a clean two-mode behavior over the entire composition range. Accordingly, the disordered system exhibits two pairs of first-order longitudinal (LO) and transverse (TO) optical modes, which are referred to as the GaAs-like and AlAs-like modes, respectively.¹ The GaAs-like (AlAs-like) modes have phonon frequencies that are related to the bulk GaAs (AlAs) parent modes. This clean division into two sets of LO-TO modes is derived essentially from the fact that there is a clear separation between the pairs of LO-TO mode

frequencies in GaAs and AlAs. By least-squares fitting all prior room-temperature Raman and infrared data,⁴⁻⁶ best fit expressions are obtained for the concentration dependences of these modes as follows:

$$\omega_{\text{TO}}^{\text{GaAs-like}}(x) = 268.16(\pm 0.61) - 11.16(\pm 3.34)x - 4.06(\pm 3.98)x^2, \quad (1)$$

$$\omega_{\text{LO}}^{\text{GaAs-like}}(x) = 292.30(\pm 0.87) - 37.46(\pm 4.48)x - 2.88(\pm 4.86)x^2, \quad (2)$$

$$\omega_{\text{TO}}^{\text{AlAs-like}}(x) = 357.48(\pm 0.69) + 4.54(\pm 1.16)x, \quad (3)$$

$$\omega_{\text{LO}}^{\text{AlAs-like}}(x) = 356.89(\pm 1.12) + 71.14(\pm 4.76)x - 26.10(\pm 4.33)x^2, \quad (4)$$

where the quantities in parentheses are the standard errors in the fits. The fit to the AlAs-like TO mode data was not improved with a quadratic expression. These expressions are similar to those obtained by Adachi¹ based on the work of Kim and Spitzer⁸ and by Feng *et al.*⁵ and Solomon *et al.*⁶ except that the quadratic term for the $\omega_{\text{LO}}^{\text{GaAs-like}}$ mode [Eq. (2)] is positive in the Adachi and Solomon *et al.* cases and absent in the case of Feng *et al.* The bowing¹ of the phonon frequencies with x is most obvious in the case of the AlAs-like LO mode. The wide spread in frequency values at a given x value^{4-6,9} indicate that although no great reliability can be placed on the mode frequencies evaluated from fits such as Eqs. (1)–(4) to the results of earlier work, the general trend with concentration is clearly evident and can be used as a bench-mark for this study.

Besides the doubling of the number of modes, alloying GaAs with AlAs introduces atomic disorder into the crystal lattice. The cationic disorder introduces a broadening of the phonon bands and their line shapes become asymmetric.^{6,10,11} In addition, the disorder allows additional features to be seen in the Raman spectrum that are not normally allowed in first-order Raman scattering such as disorder activated acoustic and optic modes.^{6,8,11-15} These modes are too weak to be observed by infrared reflectivity.⁸ It has been noted that the intensities of these disorder induced Raman bands increase in a nonlinear fashion with increasing

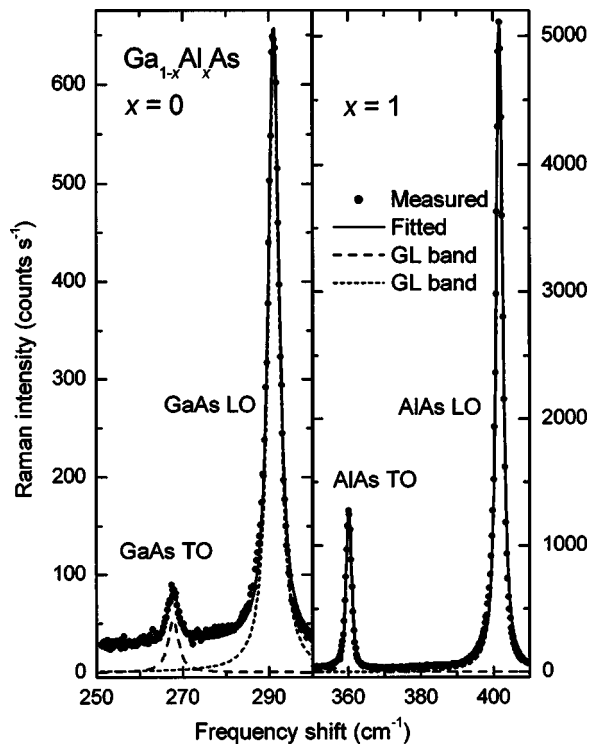


FIG. 1. Room temperature Raman spectra of $\text{Al}_x\text{Ga}_{1-x}\text{As}$ recorded with 530.9 nm excitation for undoped epilayers on GaAs(100) with $x=0$ and 1. The LO and TO curve-resolved GL peaks are shown below the spectra.

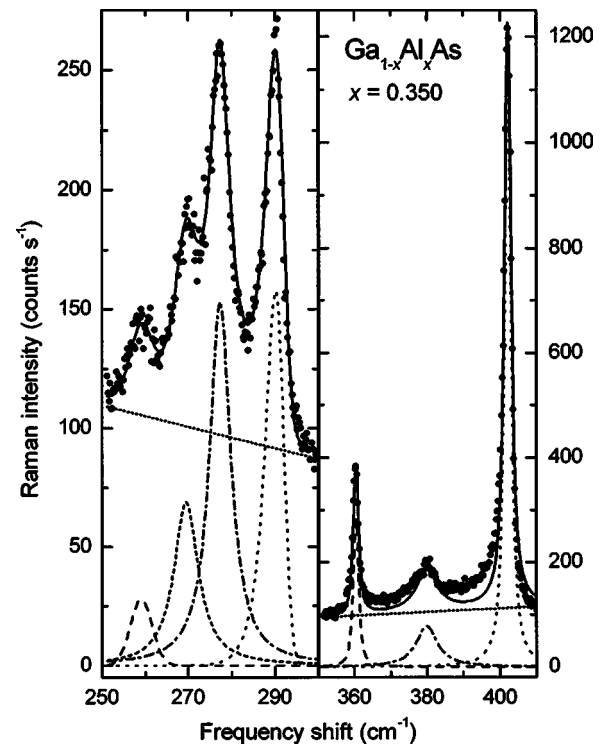


FIG. 2. Room temperature Raman spectra of $\text{Al}_x\text{Ga}_{1-x}\text{As}$ recorded with 530.9 nm excitation for $x=0.350$. The Raman line shapes have been fitted with the various component bands shown below the spectrum.

laser power⁸ and display selective resonant enhancements with a variation in the energy of the incident exciting light.¹⁶

In this paper we report on a new Raman investigation of the disordered $\text{Al}_x\text{Ga}_{1-x}\text{As}$ system using a large number of x values (an order of magnitude increase over previous studies) covering the whole concentration range and where the x values are precisely known¹⁷ eliminating a lot of the uncertainty evident in some of the previous measurements. By curve fitting the observed Raman bands detailed results are obtained for the GaAs-like and AlAs-like band parameters versus x , including a measure of the line shape asymmetry. The results obtained are compared with the predictions of various theoretical models.

II. EXPERIMENT

The samples used in this study were grown at 590 °C in a modified V80H VG-Semicon molecular beam epitaxy system.¹⁷ Each sample substrate was a 2 inch diameter (100) oriented vertical-gradient-freeze semi-insulating GaAs wafer and, in two cases, the layers were grown without substrate rotation in order to generate the desired range of alloy x values laterally across the wafer. With growth rates of 0.1(0.2) and 0.2(0.1) nm/s for GaAs and AlAs, respectively, for each wafer, x varied continuously from about 0.60(0.28) to 0.72(0.45) in the 2.5(2.0) μm thick undoped alloy layer, which was sandwiched between GaAs/AlAs calibration layers. These are the same two samples as described earlier in Ref. 17. Three other uniform samples with $x=0.197$, 0.505,

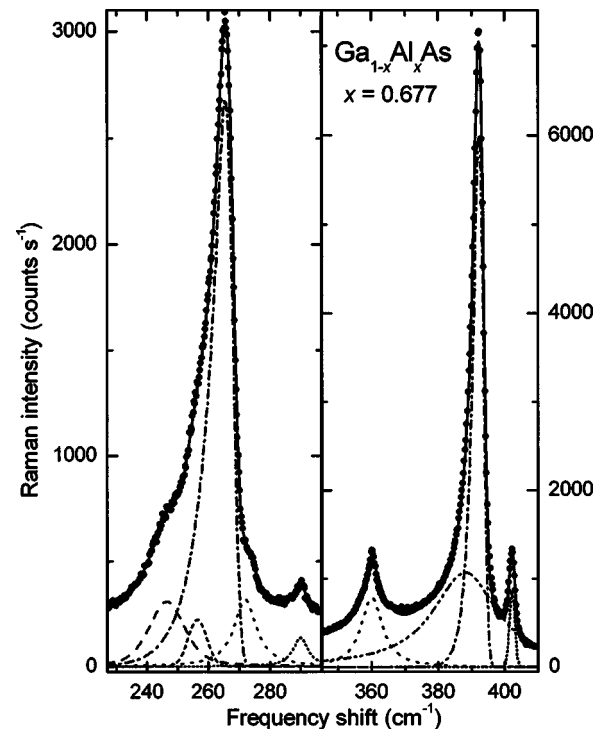


FIG. 3. Room temperature Raman spectrum of $\text{Al}_x\text{Ga}_{1-x}\text{As}$ recorded with 530.9 nm excitation for $x=0.677$. The fitted component bands are shown below the spectrum.

and 0.801 were grown using substrate rotation. The samples were measured by high resolution x-ray diffraction to map their composition (see Ref. 17 for details).

The Raman scattering experiments were carried out in an ambient atmosphere of helium at a temperature of 295 K in a quasibackscattering geometry¹⁸ with the incident light at an angle of 77.7° from the normal to the (100) surface. Spectra were excited with 300 mW of 530.9 nm krypton or 514.5 nm argon laser light, which had sufficient penetration depth to reach well into the alloy layer but not into the underlying material.¹⁷ The incident laser light formed a slit shaped spot of dimensions 1×0.1 mm² on the sample, which together with the use of the stream of He gas flowing over the sample in the laser spot area helped minimize the local laser heating. This is shown from the fact that the LO phonon frequencies thus obtained at room temperature for both GaAs and AlAs are very similar to literature values.⁴⁻⁶ The light scattered at 90° (external to the sample) was analyzed with a Spex 14018 double monochromator at a spectral resolution of 1.2 cm⁻¹, and detected with a cooled RCA 31034A photomultiplier. The incident light was polarized in the scattering plane, while the scattered light was recorded without polarization analysis. The peak frequencies of the laser line position and the strongest phonon Raman lines were obtained within 0.1 cm⁻¹ using a computer search algorithm¹⁹ and each spectrum for the $x \approx 0.3$ and 0.7

samples was frequency calibrated with respect to three reference points (the laser line zero position, the GaAs LO phonon peak, and the AlAs LO phonon peak) that covered the complete scan. For the other samples, spectrometer calibrations were made immediately before and after each alloy spectrum was recorded in the few cases where no GaAs or AlAs reference peaks were available.

III. RAMAN SPECTRA AND THEIR ANALYSIS

Representative Raman spectra for $x=0, 0.350, 0.801,$ and 1 are shown in Figs. 1–3. Sharp bands at 269 (290) and 360 (402) cm⁻¹ are the TO (LO) modes of the sample GaAs and AlAs layers, respectively (see Fig. 1). The other peaks near, but at lower frequency to, these TO-LO pairs in the alloy samples are the corresponding GaAs-like and AlAs-like TO and LO vibrational modes (see Figs. 2 and 3 and also Ref. 17). In general, the most intense bands are due to the LO modes, as the TO modes are forbidden in the backscattering geometry. The TO modes are observed weakly here because the scattering geometry is not strictly a 180° backscattering one.¹⁸ The spectra were curve resolved to reveal the individual Raman bands within the complex spectral envelopes. For most bands, the line shape was well represented by a combined Gaussian-Lorentzian (GL) model of the form

$$I_{GL}(\omega) = a_0 \frac{\left[\frac{a_3 \sqrt{\ln 2}}{a_2 \sqrt{\pi}} \exp\left(-4 \ln 2 \left(\frac{\omega - a_1}{a_2}\right)^2\right) + \frac{1 - a_3}{\pi a_2 \left(1 + 4 \left(\frac{\omega - a_1}{a_2}\right)^2\right)} \right]}{\left[\frac{a_3 \sqrt{\ln 2}}{a_2 \sqrt{\pi}} + \frac{1 - a_3}{\pi a_2} \right]}, \quad (5)$$

where a_0 =amplitude, a_1 =frequency, a_2 =width, and parameter a_3 represents the amount of Gaussian content ($a_3=0$ represents a pure Lorentzian and 1 a pure Gaussian). The Lorentzian is the natural line shape of the phonon band, but when the linewidth is resolution limited, as seen, for example, in the laser exciting line, a Gaussian is a much better representation. As can be seen from Fig. 1, this line shape is an excellent fit to the TO and LO modes for the limits of $x=0$ (GaAs) and 1 (AlAs). For the alloy, however, an asymmetry in the LO mode line shape is observed (see, for example, Fig. 3), as reported previously.^{6,10,11} To properly account for this asymmetry, an exponentially modified Gaussian (EMG) line shape was used,

$$I_{EMG}(\omega) = \frac{a_0}{2a_3} \exp\left(\frac{a_2^2}{2a_3^2} + \frac{a_1 - \omega}{a_3}\right) \times \left[\operatorname{erf}\left(\frac{\omega - a_1}{\sqrt{2}a_2} - \frac{a_2}{\sqrt{2}a_3}\right) + \frac{a_3}{|a_3|} \right], \quad (6)$$

where a_0 =area, a_1 =frequency (note that, unless the fitted

peak is symmetric, a_1 is not coincident with the frequency of the EMG function maximum), a_2 =width, and a_3 is the line shape asymmetry parameter. This last parameter is negative when the band is broadened asymmetrically to lower frequency. Using Eqs. (5) and (6), where appropriate, all Raman spectra were curve resolved in the regions of the GaAs-like and AlAs-like modes and representative results are shown in Figs. 2 and 3. Although the EMG model adequately represented the line shape of the alloy LO modes, another GL band was often required to account for a continuum of disorder-induced optical mode Raman scattering between the TO and LO modes. Including just this single additional oscillator was remarkably successful in accounting for the continuum (see, for example, Figs. 2 and 3).

Results obtained from the fits to the TO and LO bands are shown for the GaAs-like and AlAs-like mode frequencies in Figs. 4 and 5, respectively. In the case of the EMG model used for the LO modes, the frequency of the function maximum is graphed in Figs. 4 and 5 for ease of comparison with earlier work. Excellent results are obtained for the concen-

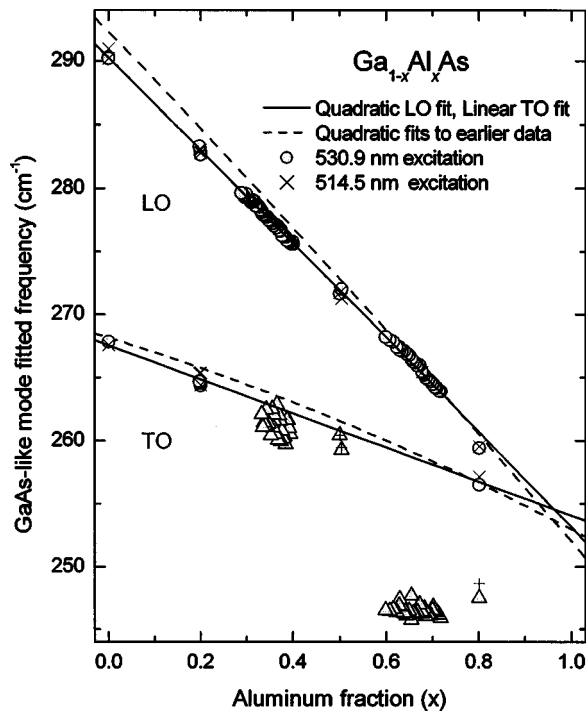


FIG. 4. Concentration dependence of fitted Raman frequencies of the GaAs-like LO and TO phonons in $\text{Al}_x\text{Ga}_{1-x}\text{As}$ at 295 K using excitation at (○) 530.9 and (×) 514.5 nm. The solid lines are least-squares fits of quadratic and linear expressions to the LO and TO data, respectively. The long dashed lines given by Eqs. (1) and (2) represent the concentration dependence of the combined earlier Raman and infrared results. Another phonon peak obtained from the fitting procedure in the vicinity of the TO phonon is indicated by triangles for 530.9 nm excitation and by plus signs for 514.5 nm excitation.

tration dependence of the frequencies of the strong LO modes, with a good consistency between data obtained from 530.9 and 514.5 nm excitation. Results for the weak AIAs-like TO band are more sparse, because this mode could either not be observed (too weak) or identified for the $x \approx 0.3$ and 0.7 samples, respectively. Similar problems occurred for the GaAs-like TO mode, where the band frequencies for the $x \approx 0.3, 0.5,$ and 0.7 samples are clearly out of line with the other data. In these samples, the weak TO mode is masked by a stronger and broader disorder-induced LO scattering that extends to lower frequency from the main GaAs-like LO mode.

A least-squares fit of polynomials to the LO and TO mode data of Figs. 4 and 5 yielded best results with

$$\omega_{\text{TO}}^{\text{GaAs-like}}(x) = 267.56(\pm 0.19) - 13.51(\pm 0.48)x, \quad (7)$$

$$\omega_{\text{LO}}^{\text{GaAs-like}}(x) = 290.25(\pm 0.12) - 36.05(\pm 0.57)x - 1.10(\pm 0.63)x^2, \quad (8)$$

$$\omega_{\text{TO}}^{\text{AIAs-like}}(x) = 359.78(\pm 0.10) + 0.46(\pm 0.11)x, \quad (9)$$

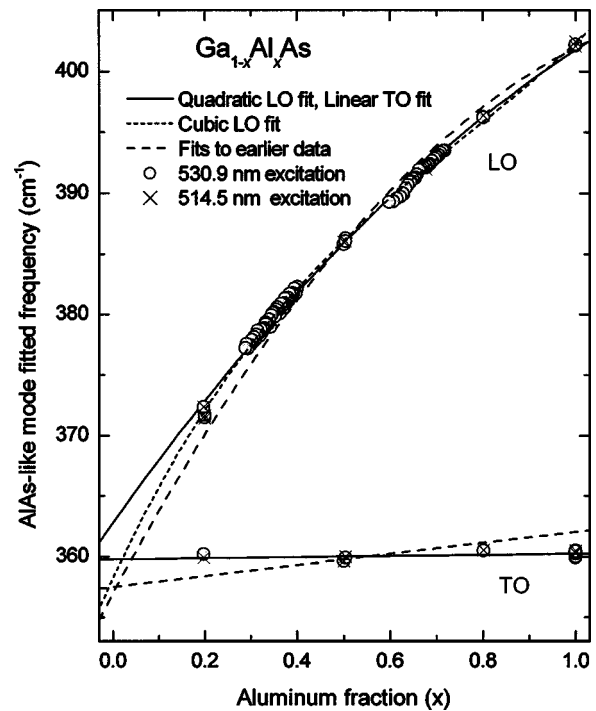


FIG. 5. Concentration dependence of fitted Raman frequencies of the AIAs-like LO and TO phonons in $\text{Al}_x\text{Ga}_{1-x}\text{As}$ at 295 K using excitation at (○) 530.9 and (×) 514.5 nm. The solid lines are least-squares fits of quadratic and linear expressions to the LO and TO data, respectively. The long dashed lines given by Eqs. (3) and (4) represent the concentration dependence of the combined earlier Raman and infrared results. The short dashed line is a fit of a cubic expression to the LO data.

$$\omega_{\text{LO}}^{\text{AIAs-like}}(x) = 362.78(\pm 0.28) + 53.34(\pm 1.11)x - 14.36(\pm 0.98)x^2. \quad (10)$$

The quantities in parentheses in Eqs. (7)–(9) are the standard deviations in the fits. For the GaAs-like TO data, the band frequencies for the $x \approx 0.3, 0.5,$ and 0.7 samples (marked by \triangle and $+$ symbols in Fig. 4) were not included in the fit. For the AIAs-like mode, a cubic expression gave a better fit to the data at lower x ($x < 0.3$) values, but was a worse fit than the quadratic expression, Eq. (10), at higher x ($x > 0.7$) values,

$$\omega_{\text{LO}}^{\text{AIAs-like}}(x) = 358.16(\pm 0.47) + 81.65(\pm 2.75)x - 65.80(\pm 4.86)x^2 + 28.31(\pm 2.65)x^3. \quad (11)$$

The present results are compared with earlier work in Figs. 4 and 5 by means of Eqs. (1)–(4). For the GaAs-like TO and LO modes and AIAs-like LO mode there is reasonable agreement between the present and past work, but the agreement is not as good for the AIAs-like TO mode. Equations (8) and (10) for the LO modes are generally similar to those reported earlier by Feng *et al.*⁵ The present results for the fitted mode frequencies [Eqs. (7)–(11)] are in accord with the results obtained from an earlier analysis of the phonon peak frequencies,¹⁷ as could be expected, except that the small slopes for the TO AIAs-like mode have opposite sign.

The concentration dependences of the two TO modes were not as well quantified in this study as the LO modes, because of the aforementioned difficulties in quantifying these modes. The results obtained from the fits to the spectra for the band indicated by the \triangle and $+$ symbols in Fig. 4 show the error that could arise from a misidentification of this band with the TO GaAs-like mode. As the TO modes are weak in Raman backscattering, a definitive infrared study is now required to further ascertain their concentration dependences.

The Raman results for the LO phonon frequency concentration dependence are the most detailed to date; with 95 and 97 values fitted for the GaAs-like and AlAs-like modes, respectively. Since there are, as yet, no experimental data for the limiting behavior of the mode frequencies as $x \rightarrow 0$ or 1,⁸ the fitted expressions Eqs. (7)–(11) may be used to estimate the frequencies of the localized modes of the $\text{Al}_x\text{Ga}_{1-x}\text{As}$ alloy. In the dilute limit, it is expected theoretically that the GaAs-like or AlAs-like TO and LO mode frequencies converge.⁷ The results given in Eqs. (7)–(10) prove experimentally that this is indeed the case. Equations (7) and (8) indicate that the localized (gap) mode of Ga in AlAs is at $253.6 \pm 2.5 \text{ cm}^{-1}$. For the AlAs-like modes, Eqs. (9) and (10) give $361.3 \pm 1.9 \text{ cm}^{-1}$ for the frequency of the localized mode of Al in GaAs. The use of Eqs. (9) and (11) gives a value of $360.0 \pm 1.4 \text{ cm}^{-1}$, which is likely more accurate because of the better fit of a cubic expression to the LO mode data at lower x values (see Fig. 5).

The concentration dependences of the integrated intensities of the GaAs-like and AlAs-like LO modes are shown in Figs. 6 and 7 for 530.9 nm excitation; the mode intensities are of a similar magnitude and are relatively insensitive to x apart from a sharp and dramatic increase near $x=0.7$. The location of a peak in the response for 514.5 nm excitation is not as obvious, as there are fewer points. The optical absorption coefficient²⁰ of $\text{Al}_x\text{Ga}_{1-x}\text{As}$ at 530.9 nm exhibits a sharp change at $x \approx 0.7$, as can be seen from Fig. 8, coincident with the variation in the E_0 band gap energy,²¹ which for $0.45 \leq x \leq 1.0$ is²²

$$E_0(x)[\text{eV}] = 1.656 + 0.215x + 1.147x^2 \quad (12)$$

and encompasses the laser excitation energies used here. Thus the peak in the integrated intensity response at $x \approx 0.7$ results from a resonance Raman enhancement of the GaAs-like and AlAs-like phonon cross sections at the E_0 energy gap.^{23,24} The Raman intensity is higher for $x \geq 0.8$ compared with $x \leq 0.2$ due to the change in absorption coefficient shown in Fig. 8.

Extreme resonance excitation has been shown to affect the optical phonon Raman line shape in GaAs/AlAs superlattices.²⁵ However, in the present¹⁷ or earlier⁹ cases for alloy epilayers, the phonon spectra show no remarkable changes apart from the peak intensity when moving from resonance to off-resonance excitation either by changing the laser wavelength or by changing the sample composition. The good agreement in Figs. 9–12 between results obtained at 514.5 nm with those using 530.9 nm excitation indicates that only the Raman intensities are compromised by resonance effects.

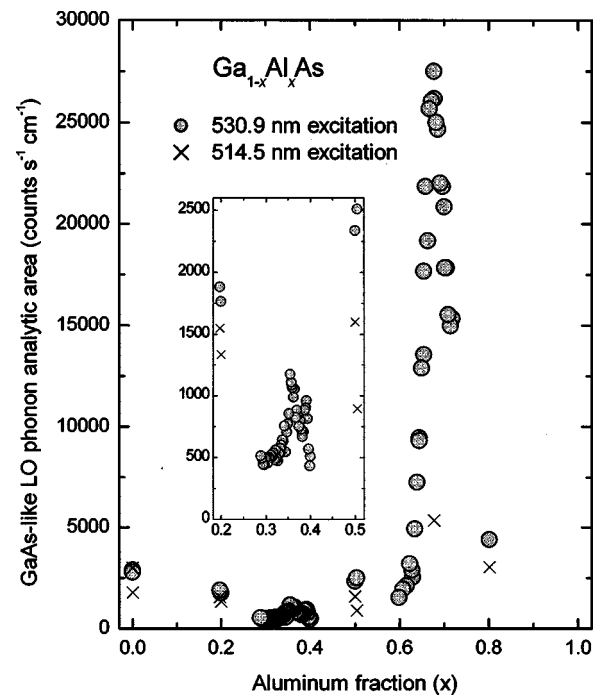


FIG. 6. The integrated intensity of the GaAs-like LO phonon of $\text{Al}_x\text{Ga}_{1-x}\text{As}$ at 295 K excited with laser lines at (O) 530.9 and (X) 514.5 nm.

The linewidth, i.e., full width at half-maximum (FWHM), of LO phonons in $\text{Al}_x\text{Ga}_{1-x}\text{As}$ is shown as a function of Al concentration in Fig. 9 for the GaAs-like mode and in Fig. 10 for the AlAs-like mode. For both modes, the FWHM is very sharp in the limit of the respective pure compound and then

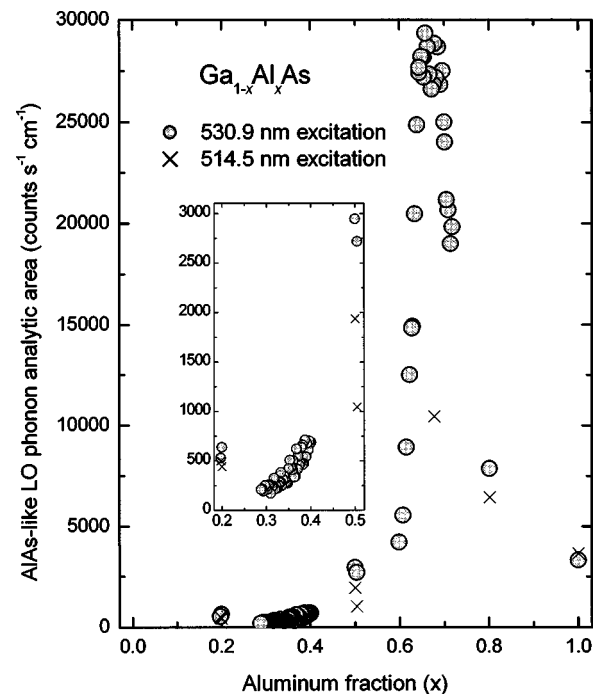


FIG. 7. The integrated intensity of the AlAs-like LO phonon of $\text{Al}_x\text{Ga}_{1-x}\text{As}$ at 295 K excited with laser lines at (O) 530.9 and (X) 514.5 nm.

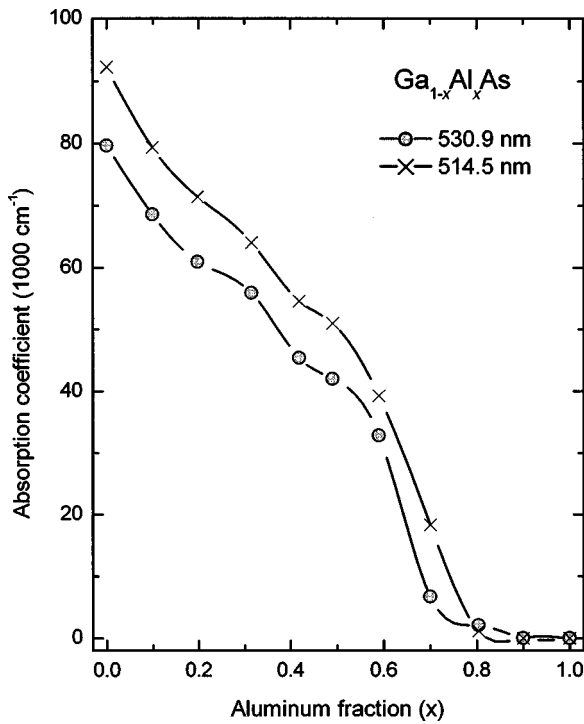


FIG. 8. The absorption coefficient of $\text{Al}_x\text{Ga}_{1-x}\text{As}$ at room temperature for wavelengths of (○) 530.9 and (×) 514.5 nm, as deduced by linear interpolation of the data from Ref. 20. The lines are guides to the eye.

increases substantially by a similar amount with increasing respective disorder. The approximately superlinear change in FWHM with x is remarkable in this system, particularly as the linewidth shows no sign of decrease at high (low) x values for the GaAs-like (AlAs-like) mode. At some point close to the respective composition limits there should be a sharp downturn in the LO phonon linewidth, as the localized mode linewidths are usually quite sharp.^{7,26}

The LO phonon asymmetry parameter for the GaAs-like and AlAs-like modes is shown as a function of x in Figs. 11 and 12, respectively. This is the first time the often observed^{6,10,11} LO phonon line shape asymmetry has been quantified. For the GaAs-like (AlAs-like) mode, the line shape becomes increasingly asymmetric to lower frequency with increasing (decreasing) x in a sublinear fashion. As for the linewidth, there is no evidence of a reversal of the trend in the mode behavior as the Al concentration approaches the respective limits of $x=0$ and 1. Again, this is a most unexpected result, as localized modes seen near the concentration limits are usually not only sharp but also symmetric.⁷ The line shape parameter behavior with x is indicative of an increasing amount of disorder-induced Raman scattering from phonons with frequencies between the first-order TO and LO modes and with wave vectors from throughout the Brillouin zone.

IV. COMPARISON WITH THEORY

There are a number of theoretical models for investigating the short wave vector vibrational properties of disordered

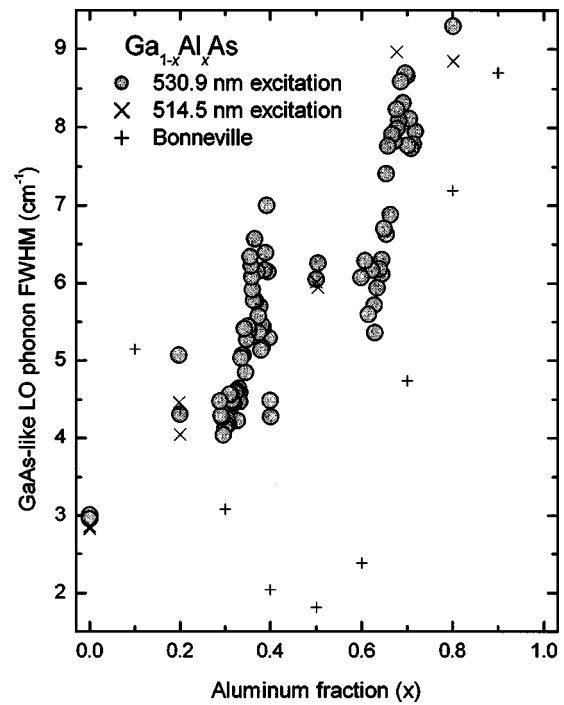


FIG. 9. The linewidth (FWHM) of the GaAs-like LO phonon of $\text{Al}_x\text{Ga}_{1-x}\text{As}$ at 295 K under excitation at (○) 530.9 and (×) 514.5 nm. Also shown are the theoretical results of Bonneville (Ref. 31) (+).

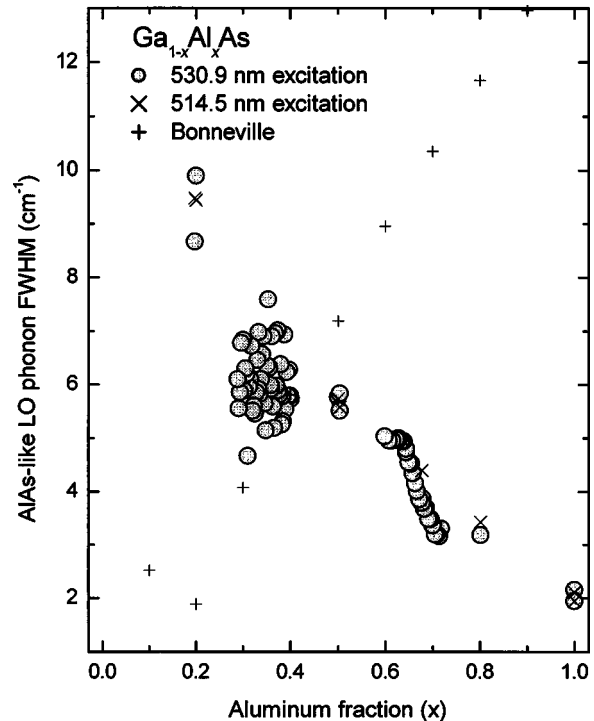


FIG. 10. The linewidth (FWHM) of the AlAs-like LO phonon of $\text{Al}_x\text{Ga}_{1-x}\text{As}$ at 295 K under excitation at (○) 530.9 and (×) 514.5 nm. Also shown are the theoretical results of Bonneville (Ref. 31) (+).

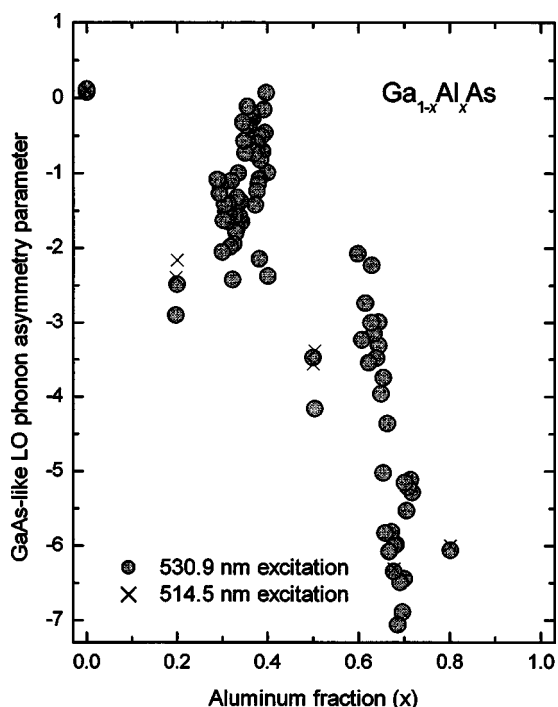


FIG. 11. The line shape asymmetry parameter for the GaAs-like LO phonon of $\text{Al}_x\text{Ga}_{1-x}\text{As}$ at 295 K under excitation at (○) 530.9 and (×) 514.5 nm.

systems.^{7,27–38} One of the oldest and most successful approaches to treating the two mode behavior of alloys is the random element isodisplacement model first developed by Chen *et al.*²⁸ and subsequently modified by a number of

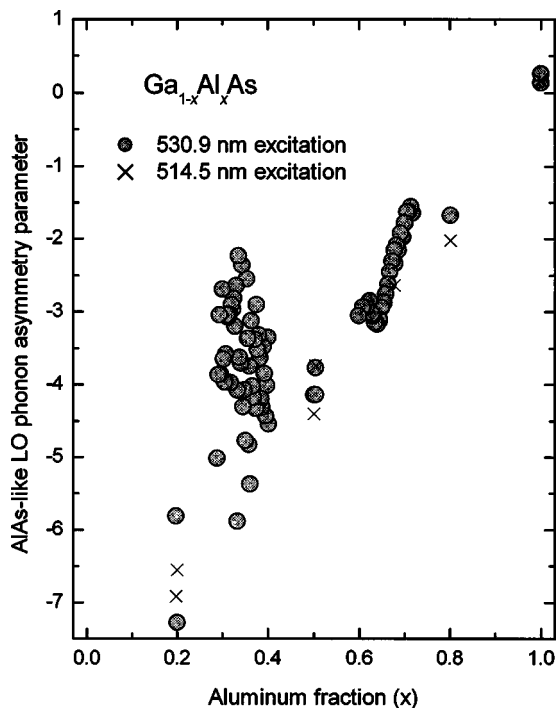


FIG. 12. The line shape asymmetry parameter for the AlAs-like LO phonon of $\text{Al}_x\text{Ga}_{1-x}\text{As}$ at 295 K under excitation at (○) 530.9 and (×) 514.5 nm.

TABLE I. Comparison of experimental and calculated values for the vibrational frequency of the isolated impurity mode in $\text{Al}_x\text{Ga}_{1-x}\text{As}$ at the limits $x \rightarrow 0$ and 1.

| Mode | Experimental (cm^{-1}) | Calculated (cm^{-1}) |
|----------------|--------------------------------------|---|
| Al (localized) | 360.0 ± 1.4 358.2 ± 0.5^f | 342^a 340^b 357^c 334^d 351.6^e |
| Ga (gap) | 253.6 ± 2.5 253.1 ± 1.3^f | 258^a 244^d 257.8^e |

^aReference 40.

^bReference 41.

^cReference 37.

^dReference 36.

^eReference 31.

^fValue obtained from extrapolation of the LO mode result alone.

authors.^{3,8,29,30} This model has been shown to be a good fit to the concentration dependence of the GaAs-like and AlAs-like TO and LO mode frequencies of $\text{Al}_x\text{Ga}_{1-x}\text{As}$.^{3,5,6,8} The fits shown in Figs. 4 and 5 given by Eqs. (7)–(10) indicate that the random element isodisplacement model is also a good fit to the present results.^{5,6} However, the model does not account for the effects of disorder represented by features such as the line shape asymmetry of the LO modes.

Lattice dynamical models have been developed that include substitutional disorder and, hence, some force constant disorder, assuming purely random alloy substitution. The approaches are generally of two types: (i) developing analytical expressions for the Green function of the alloy via the coherent potential approximation (CPA)^{31,34,39} or average transfer-matrix approximation (ATA)^{35,36} and (ii) constructing large supercells wherein the Group III atoms are randomly distributed over the cationic sublattice.^{33,37,38} An excellent review of this work on disorder effects, and its limitations, has been given by Jusserand.⁴

First we compare the theoretical predictions of these models with the experimental results for the localized and gap modes in $\text{Al}_x\text{Ga}_{1-x}\text{As}$. The comparison is made in Table I, which gives the extrapolated experimental results in two forms: the result given earlier for the intersection of the TO and LO modes, and the value obtained just from extrapolation of the LO mode data alone, which fitwise is more accurate. The theoretical results are from linear diatomic-chain,⁴⁰ CPA-shell,⁴¹ *ab initio*-supercell,³⁷ ATA,³⁶ and CPA-virtual-crystal-approximation³¹ models. Of these, the most realistic model is the *ab initio*-supercell calculation of Baroni *et al.*,³⁷ and their model produces very good agreement with experiment for the localized and gap modes. The CPA calculation of Bonneville³¹ is also in close agreement with experiment, particularly for the gap mode. The concentration dependence of the mode frequencies calculated with these two models is compared with experiment in Fig. 13. In general, there is good agreement between theory and experiment for the overall trends in the concentration dependence of the mode frequencies, but there are discrepancies between them with regard to the precise value for the frequencies. The latter could be expected, because of approximations made in the model calculations.^{31,37} Also, in this and previous work,

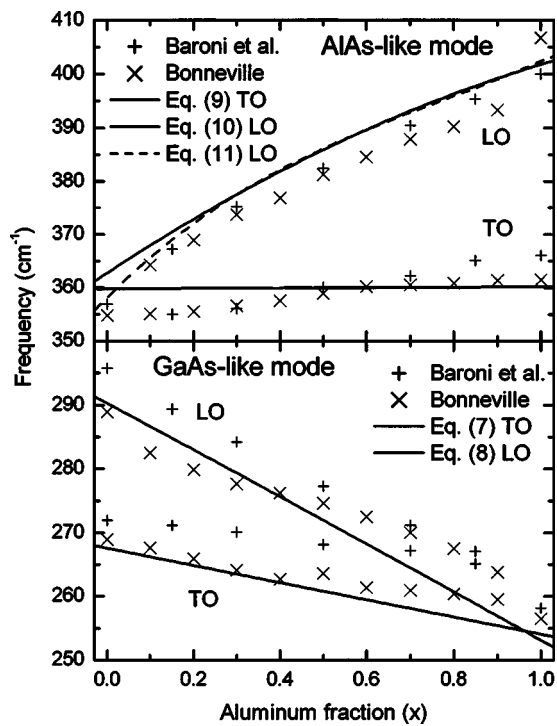


FIG. 13. Comparison of the theoretical predictions of Baroni *et al.* (Ref. 37) (+) and Bonneville (Ref. 31) (×) with the observed concentration dependences of the LO and TO modes of $\text{Al}_x\text{Ga}_{1-x}\text{As}$.

no account is taken of strain in alloy epilayers grown on GaAs(100). The AlAs lattice constant is slightly greater than that of GaAs, leading to a small lattice mismatch of 1.424×10^{-3} (Ref. 17). The effect of such a mismatch-induced strain would be to shift the phonon frequencies of an AlAs or alloy epilayer to lower frequency. Unfortunately, the phonon deformation potentials for AlAs are unknown,⁴² but based on those of GaAs, GaSb, and AlSb, which have quite similar phonon deformation potentials,⁴² a strained epilayer of AlAs on GaAs(100) would lead to optical phonon frequency shifts of less than -1 cm^{-1} . The downshifts in frequency for $\text{Al}_x\text{Ga}_{1-x}\text{As}$ would be proportionally less than for $x=1$, depending on x .

Only Bonneville³¹ has provided detailed predictions for the concentration dependence of the linewidths of the GaAs-like and AlAs-like TO and LO modes. His predictions within the CPA model for the LO modes are compared with experiment in Figs. 9 and 10. The theory is in remarkable agreement with experiment for the GaAs-like mode when allowance is made for the fact that the experimental data have not been corrected for the instrumental resolution of 1.2 cm^{-1} . For the AlAs-like mode, however, theory predicts the opposite behavior with x from that observed experimentally. The *ab initio* calculations of Baroni *et al.*³⁷ predict a linewidth of $\sim 10 \text{ cm}^{-1}$ for the optic mode at $x=0.5$, which is considerably in excess of the experimental values. Clearly, even the best of the present theories need improvement with regard to the predictions of the phonon damping.

Although several theories have reproduced the asymmetry observed in the Raman line shape,^{31,37,41} there are, so far, no quantitative results to compare with the experimental data given in Figs. 11 and 12.

V. CONCLUSIONS

Despite the fact that the lattice vibrations near zero wave vector in $\text{Al}_x\text{Ga}_{1-x}\text{As}$ are now well known and fairly well understood in comparison with other III-V semiconductor alloys, this study has shown that principal features of the Raman spectrum still lack a detailed quantitative understanding. In particular, more sophisticated three-dimensional lattice dynamics models, as noted by Jusserand,⁴ are required to explain, in this case, the concentration dependence of the optical-phonon Raman line shapes (asymmetry) and widths. Even though present theories are able to determine the localized and gap modes frequencies of $\text{Al}_x\text{Ga}_{1-x}\text{As}$ quite precisely, more theoretical effort is still required in order to reproduce these latest experimental results for the mode frequency versus x behavior.

ACKNOWLEDGMENTS

The authors thank H.J. Labbé for technical assistance in the Raman measurements and R. Radomski for the peak fitting work.

*Electronic address: david.lockwood@nrc.ca

¹S. Adachi, *J. Appl. Phys.* **58**, R1 (1985).

²*Properties of Aluminium Gallium Arsenide*, edited by S. Adachi (IEE, London, 1993).

³M. Ilegems and G.L. Pearson, *Phys. Rev. B* **1**, 1576 (1970).

⁴B. Jusserand, in *Properties of Aluminium Gallium Arsenide*, edited by S. Adachi (IEE, London, 1993), pp. 30–35.

⁵Z.C. Feng, S. Perkowitz, D.K. Kinell, R.L. Whitney, and O.N. Talwar, *Phys. Rev. B* **47**, 13 466 (1993).

⁶G.S. Solomon, D Kirillov, H.C. Chui, and J.S. Harris, Jr., *J. Vac. Sci. Technol. B* **12**, 1078 (1994).

⁷A.S. Barker, Jr. and A.J. Sievers, *Rev. Mod. Phys.* **47**, S1 (1975).

⁸O.K. Kim and W.G. Spitzer, *J. Appl. Phys.* **50**, 4362 (1979).

⁹N. Saint-Cricq, G. Landa, J.B. Renucci, I. Hardy, and A. Munoz-Yague, *J. Appl. Phys.* **61**, 1206 (1987).

¹⁰P. Parayanthal and F.H. Pollak, *Phys. Rev. Lett.* **52**, 1822 (1984).

¹¹B. Jusserand and J. Sapriel, *Phys. Rev. B* **24**, 7194 (1981).

¹²R. Tsu, H. Kawamura, and L. Esaki, in *Proceedings of the International Conference on Physics of Semiconductors* (Elsevier, Amsterdam, 1972), Vol.2, p. 1135; H. Kawamura, R. Tsu, and L. Esaki, *Phys. Rev. Lett.* **29**, 1397 (1972).

¹³J. Shah, A.E. DiGiovanni, T.C. Damen, and B.I. Miller, *Phys. Rev. B* **7**, 3481 (1973).

¹⁴A.S. Barker, Jr., J.L. Merz, and A.C. Gossard, *Phys. Rev. B* **17**, 3181 (1978).

¹⁵N. Saint-Cricq, R. Carles, J.B. Renucci, A. Zwick, and M.A. Re-

- nucci, *Solid State Commun.* **39**, 1137 (1981).
- ¹⁶R. Carles, N. Saint-Cricq, A. Zwick, M.A. Renucci, and J.B. Renucci, *Nuovo Cimento D* **2**, 1712 (1983).
- ¹⁷Z.R. Wasilewski, M.M. Dion, D.J. Lockwood, P.J. Poole, R.W. Streater, and A.J. SpringThorpe, *J. Appl. Phys.* **81**, 1683 (1997); D.J. Lockwood, R. Radoski, and Z.R. Wasilewski, *J. Raman Spectrosc.* **33**, 202 (2002); D.J. Lockwood and Z.R. Wasilewski, *Solid State Commun.* **126**, 261 (2003).
- ¹⁸D.J. Lockwood, M.W.C. Dharma-wardana, J.-M. Baribeau, and D.C. Houghton, *Phys. Rev. B* **38**, 2243 (1987).
- ¹⁹J.W. Arthur, *J. Raman Spectrosc.* **5**, 2 (1976).
- ²⁰S. Adachi, in *Properties of Aluminium Gallium Arsenide*, edited by S. Adachi (IEE, London, 1993), p. 125.
- ²¹F.H. Pollak, in *Properties of Aluminium Gallium Arsenide*, edited by S. Adachi (IEE, London, 1993), p. 53.
- ²²H.C. Casey and M.B. Panish, *Heterostructure Lasers* (Academic, New York, 1978), Part A, p. 193.
- ²³M. Cardona, in *Light Scattering in Solids II*, edited by M. Cardona and G. Güntherodt (Springer, Berlin, 1982), Chap. 2.
- ²⁴R. Trommer and M. Cardona, *Phys. Rev. B* **17**, 1865 (1978).
- ²⁵G.S. Spencer, J. Menéndez, L.N. Pfeiffer, and K.W. West, *Solid State Commun.* **97**, 21 (1996).
- ²⁶W. Hayes and R. Loudon, *Scattering of Light by Crystals* (Wiley, New York, 1978), p. 131.
- ²⁷I.F. Chang and S.S. Mitra, *Adv. Phys.* **20**, 359 (1971).
- ²⁸Y.S. Chen, W. Shockley, and G.L. Pearson, *Phys. Rev.* **151**, 648 (1966).
- ²⁹I.F. Chang and S.S. Mitra, *Phys. Rev.* **172**, 924 (1968); *Phys. Rev. B* **2**, 1215 (1970).
- ³⁰H. Harada and S. Narita, *J. Phys. Soc. Jpn.* **30**, 1628 (1971).
- ³¹R. Bonneville, *Phys. Rev. B* **24**, 1987 (1981); **29**, 907 (1984).
- ³²C.W. Myles, *Phys. Rev. B* **28**, 4519 (1983).
- ³³M.J. O'Hara, C.W. Myles, and J.D. Dow, *J. Phys. Chem. Solids* **42**, 1043 (1981).
- ³⁴P.N. Sen and W.M. Hartmann, *Phys. Rev. B* **9**, 367 (1974).
- ³⁵P.N. Sen and G. Lucovsky, *Phys. Rev. B* **12**, 2998 (1975).
- ³⁶M. Bernasconi, L. Colombo, L. Miglio, and G. Benedek, *Phys. Rev. B* **43**, 14 447 (1991).
- ³⁷S. Baroni, S. de Gironcoli, and P. Giannozzi, *Phys. Rev. Lett.* **65**, 84 (1990).
- ³⁸P. Pavone, B. Steininger, and D. Strauch, *Comput. Mater. Sci.* **20**, 363 (2001).
- ³⁹D.W. Taylor, *Phys. Rev.* **156**, 1017 (1967).
- ⁴⁰G. Lucovsky, M.H. Brodsky, and E. Burstein, *Phys. Rev. B* **2**, 3295 (1970).
- ⁴¹B. Jusserand, D. Paquet, and K. Kunc, in *Proceedings of the 17th International Conference on Physics of Semiconductors*, edited by J.D. Chadi and W.A. Harrison (Springer, New York, 1985), p. 1165.
- ⁴²A. Anastassakis, in *Light Scattering in Semiconductor Structures and Superlattices*, edited by D.J. Lockwood and J.F. Young (Plenum, New York, 1991), p. 173.